Supplementary Material

A polymer surfactant corona dynamically replaces water in solvent-free protein liquids and ensures macromolecular flexibility and activity

François-Xavier Gallat[&,#,$,◊,+], Alex P.S. Brogan[&,%], Yann Fichou[#,$,◊], Nina McGrath[%], Martine Moulin[+,ß], Michael Härtlein[+,ß], Jérôme Combet[+], Joachim Wuttke[‡], Stephen Mann[%], Giuseppe Zaccai[#,$,◊,+], Colin J. Jackson[ƒ], Adam W. Perriman[*,%] and Martin Weik[*,#,$,◊,±]

[#]Comissariat à l'Energie Atomique, Institut de Biologie Structurale, F-38054 Grenoble, France

[$]CNRS, UMR5075, F-38027 Grenoble, France

[◊]Université Joseph Fourier, F-38000, Grenoble, France

[+]Institut Laue-Langevin, 6 rue Jules Horowitz, B.P. 156, 38042 Grenoble Cedex 9, France

[%]Center for Organized Matter Chemistry, School of Chemistry, University of Bristol, Bristol BS8 1TS, UK

[ß]ILL-EMBL Deuteration Laboratory, Partnership for Structural Biology, Grenoble

[‡]Forschungszentrum Jülich, JCNS at FRM II, Lichtenbergstrasse 1, 85747 Garching, Germany

[ƒ]Research School of Chemistry, Australian National University, ACT, 0200, Australia

[±]ESRF, 6 rue Jules Horowitz, BP 220, 38043 Grenoble Cedex, France.

F.-X. Gallat and A.P.S. Brogan contributed equally.

Correspondence : weik@ibs.fr, chawp@bristol.ac.uk

1. Supporting Materials and Methods

1.1 Myoglobin deuteration, purification and characterization

Deuterated sperm whale myoglobin (DMb) (see sequence below) was produced in the ILL-EMBL Deuteration Laboratory with an N-terminal hexahistidine tag using pET28a (Novagen) as expression vector. *E. coli* BL21(DE3) cells transformed with pET28myo were grown to high cell density in a fermentation process using fully deuterated Enfors minimal medium. When an optical density (OD_{600nm}) of 10 was reached, cells were induced with 0.5 mM IPTG for protein expression. Bacteria were harvested at an OD_{600nm} value of 17 corresponding to 70 g of bacterial cell paste from 1.7L. Protein purification was achieved in one step using immobilized cobalt ion affinity chromatography. Cell lysis was carried out by sonication in a buffer containing 20 mM Tris-HCl, pH 8.0 and 500 mM NaCl (lysis buffer). After centrifugation the supernatant was incubated at 8°C with the cobalt resin under stirring for 1 hour. The resin was then transferred to a column and washed with lysis buffer containing 8 mM imidazole. DMb was eluted with the lysis buffer containing 250 mM imidazole. The pooled fractions were subsequently dialysed against 20 mM Tris-HCl, pH 8.0, 50 mM NaCl. Protein purity was assessed by 12% Tris-Tricine SDS PAGE. Lyophilised horse myoglobin was purchased from Sigma-Aldrich (M0630) and used without further purification.

Sperm whale myoglobin sequence:

MGSSHHHHHHSSGLVPRGSHMVLSEGEWQLVLHVWAKVEADVAGHGQDILIRLFKSHPE
TLEKFDRFKHLKTEAEMKASEDLKKHGVTVLTALGAILKKKGHHEAELKPLAQSHATKHK
IPIKYLEFISEAIIHVLHSRHPGNFGADAQGAMNKALELFRKDIAAKYKELGYQG

Horse myoglobin sequence:

MGLSDGEWQQVLNVWGKVEADIAGHGQEVLIRLFTGHPETLEKFDKFKHLKTEAEMKAS
EDLKKHGTVVLTALGGILKKKGHHEAELKPLAQSHATKHKIPIKYLEFISDAIIHVLHSKHP
GDFGADAQGAMTKALELFRNDIAAKYKELGFQG

UV-Vis absorption spectroscopy was employed to estimate the ratio between the holo- and apo-forms of DMb. Spectra were recorded from 200 to 700 nm on solutions of DMb in H_2O and of hydrogenated horse myoglobin (HMb) in H_2O (Figure SI Methods 1). It was assumed that hydrogenated horse myoglobin was fully in its holo form. The ratio $absorbance_{410nm}$ (DMb)/ $absorbance_{280nm}$ (DMb) then indicated DMb was 35 % in the holo- and 65 % in the apo-form.

SAXS experiments[1] have revealed only small differences in the radii of gyration of holo (18 Å) and apo Mb (20 Å) and incoherent neutron scattering experiments have shown very similar ns – ps dynamics for holo- and apo-Mb[2]. Consequently, apo- and holo-Mb can be considered as being

structurally and dynamically very similar and we conclude that different apo/holo ratios for DMb and for HMb do not affect the ns-ps dynamics of the hybrids and the polymer moieties.

1.2 Synthesis and characterization of anionic polymer surfactants

Tempo-mediated oxidation of the terminal hydroxyl group of polyoxyethylene lauryl ether to yield glycolic acid ethoxylate lauryl (HS_5**)** ether was undertaken using a previously reported method[3] with minor modifications. Briefly, 2 g of polyoxyethylene lauryl ether (Brij l23, Sigma-Aldrich) was dissolved in water (50 ml) with NaBr (516 mg), TEMPO (52 mg) and NaClO (5 ml, available chlorine 10-15%). The solution was adjusted to pH 11 and maintained while stirring for 24 hours. The oxidation was quenched by the addition of 10 ml of ethanol, followed by acidification with HCl to pH 1 and extraction with 3 x 80 ml aliquots of chloroform. The $CHCl_2$ layers were combined and dried under reduced vacuum. The resulting pale yellow oil was redissolved in 50 ml hot ethanol followed by precipitation in the freezer overnight. Removal of the supernatant ethanol followed by a subsequent recrystallization with ethanol and drying under vacuum gave glycolic acid ethoxylate lauryl as a colourless waxy solid in 70% yield. NMR spectra were recorded at ambient temperatures on a Varian 500 (^{1}H: 499.9 MHz, ^{13}C: 125.7 MHz) spectrometer with all resonances referenced to residual NMR solvent resonances. The ^{13}C NMR spectrum of polyoxyethylene lauryl showed a peak at 61.84 ppm from the carbon adjacent to the terminal hydroxyl group (Figure SI Methods 2), and oxidation to the corresponding acid resulted in the loss of this peak and the formation of a peak at the 171.85 ppm (carboxylate carbon) (Figure SI Methods 2). ^{1}H NMR also showed effective oxidation with the formation of a peak at 4.16 ppm (Figure SI Methods 3) that corresponded to the protons on the α-carbon to the carboxylate. FTIR spectra (Perkin Elmer Spectrum 1 spectrometer equipped with a diamond probe) also showed the appearance of a strong carbonyl stretch at 1740 cm^{-1} after oxidation (Figure SI Methods 4). Gel permeation chromatography (Viscotek VE 2001 with a VE 3580 refractometer) gave traces with almost identical retention volumes and widths before and after oxidation (Figure SI Methods 5) signifying no change in the polydispersity of the polymer after oxidation. Matrix-assisted laser desorption ionization (MALDI) mass spectrometry (Figure SI Methods 6) gave a number average molecular weight (M_n) of 1274 Da with a polydispersity index (PDI) of 1.07. Alpha-deuterated tridecanol propionic acid terminated deuterated poly(ethylene glycol) (DS_5) was synthesized by Polymer Source (Polymer Source Inc., Montreal, Canada) using anionic living polymerization of deuterated ethylene oxide, and MALDI mass spectrometry (Figure SI Methods 7) gave a M_n of 1444 Da with a PDI of 1.03. For poly(ethylene glycol) 4-nonylphenyl 3-sulfopropyl ether (HS_1) (Sigma-Aldrich, 473197), MALDI mass spectrometry (Figure SI Methods 8) gave a M_n of 1198 Da with a PDI of 1.03.

1.3 Myoglobin functionalization and polymer grafting

Solvent-free protein polymer surfactant nano hybrids (hereafter referred to as 'hybrids') of deuterated sperm whale myoglobin and hydrogenated horse myoglobin were synthesized using a method reported previously[4]. Briefly, nucleophilic addition of *N,N'*-dimethyl-1,3-propanediamine (DMPA) to the acid side chains of the myoglobins was achieved via carbodiimide activation, and the resulting solutions dialysed against milli-Q quality water for 48 hours. MALDI-TOF mass spectroscopy (Applied Biosystems, 4700 Proteomics analyser) was used to calculate the cationization efficiency and hence the number of DMPA molecules bound per protein molecule, which was 95% (20 DMPA molecules) and 86% (18 DMPA molecules) for horse and deuterated sperm-whale myoglobin respectively. The resulting cationized protein solutions were then added slowly to an excess of the relevant anionic polymer (HS_1, HS_5 or DS_5), stirred for 12 hours and then dialysed against milli-Q quality water (H_2O) for 48 hours to remove unbound surfactant. The samples were then lyophilised for 72 hours to yield a red waxy solid. Samples containing the hydrogenous polymer surfactants (HS_1 and HS_5) melted after annealing at 50°C to produce solvent-free myoglobin liquids, and samples produced using DS_5 did not form a liquid but instead collapsed on melting to produce a fibrous solid. Thermogravimetric (TGA) analysis of the solvent free liquid comprising cationized horse myoglobin and the surfactant HS_5 gave a water content of 0.0035 g H_2O/g myoglobin hybrid (Figure SI Methods 9).

1.4 Sample preparation for neutron scattering and relative contributions of the sample components to the incoherent scattering signal

Five different samples were prepared: cationized, hydrogenated horse myoglobin complexed with the hydrogenated polymer surfactant HS_1 (HMb/HS_1; see Figure 1b for chemical structures of the polymer surfactants); cationized, hydrogenated horse myoglobin complexed with the hydrogenated polymer surfactant HS_5 (HMb/HS_5); cationized, hydrogenated horse myoglobin complexed with the deuterated polymer surfactant DS_5 (HMb/DS_5); cationized, deuterated sperm-whale myoglobin complexed with the hydrogenated polymer surfactant HS_5 (DMb/HS_5); and hydrogenated horse myoglobin powder, hydrated with D_2O to a level of 0.43 g D_2O / g Mb (HMb/D_2O). The four hybrid samples, *i.e.* HMb/HS_1, HMb/HS_5, HMb/DS_5, DMb/HS_5 had total masses of 177 mg, 142 mg, 334 mg, and 253 mg, respectively, and were dried over P_2O_5 for 24 h on 4×3 cm^2 flat aluminium sample holders and then sealed by an aluminium cover (0.3 mm neutron path length) and a 1 mm indium seal.

For preparation of the HMb/D_2O sample, 125 mg of horse myoglobin as purchased (see above for sequence and source) was dried over P_2O_5 for 24 h on a 4×3 cm^2 flat aluminium sample holder. The resulting hydration level was defined as corresponding to 0 g water / g Mb. It has been

reported that such a drying procedure removes all but four tightly bound structural water molecules from lysozyme[5]. The dry Mb powder was then rehydrated through the vapour phase over 100% D_2O. When a final weight corresponding to a hydration level of 0.43 g D_2O /g HMb (corresponding to 0.4 g H_2O/g hydrogenated protein or 386 water molecules) was reached, the sample was sealed by an aluminium cover (0.3 mm neutron path length) and a 1 mm indium seal. After the neutron experiment, the HMb/D_2O sample was opened, dried over P_2O_5 for 24 h and sealed again (HMb-dry sample) for subsequent neutron scattering.

If one assumes that none of the exchangeable hydrogens in HMb and all exchangeable deuterons in DMb, *i.e.* 19% of all hydrogens/deuterons in the protein, exchanged, and that there are i) 41 polymer surfactant chains and 20 DMPA linkers per Mb molecule in the hybrids HMb/HS_1 and HMb/HS_5, ii) 41 polymer surfactant chains and 18 DMPA linkers per Mb molecule in the hybrid DMb/HS_5, iii) 18 polymer surfactant chains and 20 DMPA linkers per Mb molecule in the hybrid HMb/DS_5, the following contributions to the total incoherent scattering cross section of the samples are calculated:

HMb/HS_1: 26% from the cationized hydrogenated horse Mb (120,425 barn; 1 barn = 10^{-24} cm^2) and 74% from the polymer surfactant corona (344,072 barn).

HMb/HS_5: 23% from the cationized hydrogenated horse Mb (120,425 barn) and 77% from the polymer surfactant corona (393,149 barn).

DMb/HS_5: 11% from the cationized deuterated sperm whale Mb (49,692 barn) and 89% from the polymer surfactant corona (393,149 barn).

HMb/DS_5: 91% from the cationized hydrogenated horse Mb (120,425 barn) and 9% from the polymer surfactant corona (11,700 barn).

HMb/D_2O: 98% from the hydrogenated horse Mb (97,670 barn) and 2% from the D_2O hydration water (1,577 barn).

HMb-dry: 100% from the hydrogenated horse Mb (97,670 barn).

1.5 Elastic incoherent neutron scattering experiments and data processing

Elastic incoherent neutron scattering experiments were performed on HMb/HS_5, HMb/DS_5, DMb/HS_5, HMb/D_2O and HMb-dry using the backscattering spectrometer IN16[6] (Institut Laue Langevin, Grenoble, France) with an energy resolution of 0.9 μeV (full width at half maximum of the elastic peak), a wavelength of 6.271 Å and an accessible Q-range of 0.02-1.9 $Å^{-1}$. These instrument characteristics give access to motions faster than 1 ns and on the Å length scale. Samples were introduced into an *orange* ILL cryostat at room temperature at an angle of 135º with respect to the incident neutron beam and the temperature was lowered in 2 hours to 20 K. Elastically scattered neutrons were recorded while the temperature was continuously increased from 20 to 300 K. The rates of temperature increase were i) 0.24 K/min for the HMb/HS_5 sample ii) 0.15 K/min for the HMb/DS_5 sample iii) 0.14 K/min for the DMb/HS_5 sample, iv) 0.20 K/min for the HMb/D_2O sample and v) 0.19 K/min for the HMb-dry sample. Mean square displacement (MSD) $<u^2>$ of motions resolved by the spectrometer were calculated from the Q-dependence of the elastic intensity according to the Gaussian approximation:

$$I(Q,\omega=0) = A_0 \exp(-\frac{1}{6} < u^2 > Q^2) \qquad (1)$$

that is valid for:

$$Q^2 < u^2 > < 2 \qquad (2)$$

where $I(Q,\omega=0)$ is the elastically-scattered intensity and A_0 is the value of the scattering intensity at $Q = 0$. The $<u^2>$ defined by eq. (1) corresponds to the full amplitude of the motion and not to the displacement from an equilibrium position. The elastic intensity at a given temperature was corrected for detector efficiencies and normalized to the elastic intensity at 20 K. MSD were extracted in the range $0.20 < Q^2 < 1.40$ $Å^{-2}$ for the HMb/HS_5, HMb/DS_5, HMb/D_2O samples, in the range $0.18 < Q^2 < 1.33$ $Å^{-2}$ for the HMb-dry sample, and in the range $0.20 < Q^2 < 1.13$ $Å^{-2}$ for the DMb/HS_5 sample (Figure SI Methods 10). MSD of the HMb/D_2O sample have been published before[7].

Elastic incoherent neutron scattering experiments on HMb/HS_1 were performed on the backscattering spectrometer SPHERES[8] (Jülich Centre for Neutron Science at FRMII, Garching, Germany) with an energy resolution of 0.6 μeV (full width at half maximum of the elastic peak), a wavelength of 6.271 Å and an accessible Q-range of 0.2-1.9 $Å^{-1}$. Experiments and data analysis were performed in the same way than the above-described experiments on IN16, with the

exceptions of the rate of temperature increase (0.23 K/min for the HMb/HS_1) and the Q^2 range over which MSD were extracted ($0.3 < Q^2 < 1.30$ Å $^{-2}$).

1.6 Synchrotron radiation circular dichroism spectroscopy and thermal denaturation thermodynamics

Synchrotron radiation circular dichroism (SRCD) experiments were performed at the Diamond Light Source on beamline B23. Spectra were collected over a wavelength range of 260 to 165 nm with an integration time of 1 second and the temperature was controlled using a modified Linkam thermal stage with a sample cell comprising two synthetic quartz plates. Spectra were collected between 25 and 225°C at 10°C intervals and allowed to equilibrate for 5 minutes at a given temperature. The sample path length was estimated using the mass and surface area of the sample. SRCD data were deconvoluted using DICHROWEB[9] with the CDSSTR algorithm[10] and associated data set[11,12] to give the relative fractions of secondary structure where all normalized root mean square deviations of resultant fits did not exceed 0.055.

Thermodynamic parameters were evaluated by applying a two-state model to the thermal denaturation data[13-15]:

$$N \overset{K_D}{\rightleftharpoons} D \tag{3}$$

where N is the native state, D is the denatured state, and K_D is the equilibrium constant.
The intensity of the negative circular dichroic peak at 222 nm was used as the order parameter (y) to express the fraction denatured (f_D),

$$f_D = \frac{(y - y_N)}{(y_D - y_N)} \tag{4}$$

where y_N and y_D are defined as the 222 nm peak intensity in the native and denatured state respectively.

The fraction denatured can now be expressed as:

$$K_D = \frac{f_D}{1 - f_D} \tag{5}$$

and the Gibbs free energy of denaturation (ΔG_D) evaluated using equilibrium constant:

$$\Delta G_D = -RT \ln K_D \quad (6)$$

Finally, ΔG_D was plotted as a function of temperature and the transition region was fitted using linear regression yielding the half-denaturation temperature (T_m) where $\Delta G_D = 0$.

1.7 Oxygen binding assays

Oxygen binding assays were performed using a method described previously[4]. Briefly, deoxygenated hybrids were produced by dialysing cationised met-myoglobin against degassed Milli-Q water containing 0.06M $Na_2S_2O_4$ under a continuous nitrogen purge followed by electrostatic complexation with surfactant HS_5, and the resultant conjugate was dialysed under the same reducing conditions for a further 48 hours. The solution was lyophilized for 48 hours and heated to 60°C in a dry environment under nitrogen to yield the corresponding deoxyhybrid (deoxy HMb/HS_5) and stored under a dry nitrogen atmosphere.

O_2 binding experiments were undertaken by applying a film of deoxy HMb/HS_5 to the interior of a glass cell fitted with a Youngs tap under a nitrogen environment and O_2 partial pressures were measured using a Pirani gauge. Gaussian functions were fitted to the Soret bands from DR-UV-Vis spectra collected at different partial O_2 pressures, to yield the peak wavelength (λ) which was used as an order parameter to define the fraction of oxygen saturation, Y:

$$\lambda_{obs} = Y\lambda_{sat} + (1-Y)\lambda_{free} \quad (7)$$

where λ_{obs} is the wavelength of the Soret band peak, λ_{sat} is the Soret band peak wavelength at oxygen saturation, and λ_{free} is the Soret band peak wavelength for deoxy-Mb.

Finally, the Hill coefficient, h, and the oxygen affinity, $P_{1/2}$, were determined using the using the Hill equation:

$$Y = \left[1 + \left(\frac{P_{1/2}}{P}\right)^h\right]^{-1} \quad (8)$$

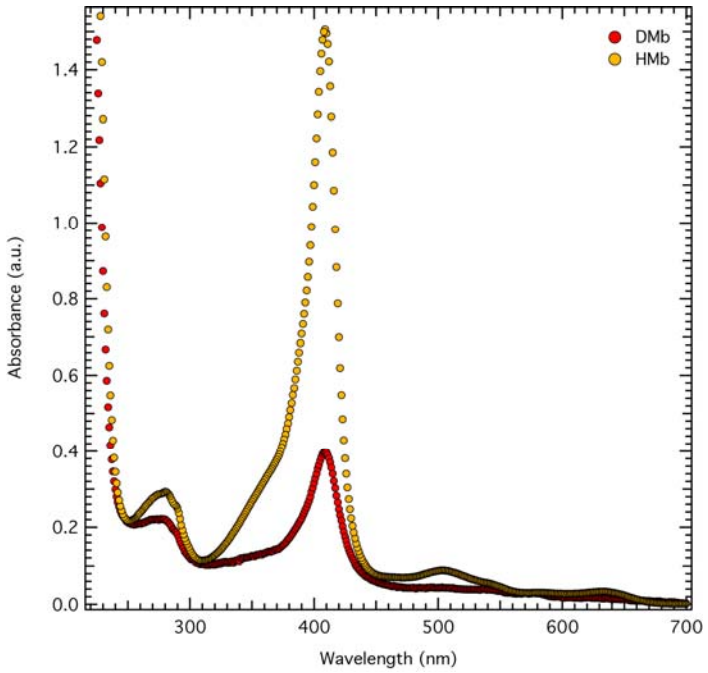

Figure SI Methods 1. UV-Vis spectra recorded from 200 to 700 nm for the deuterated (red) and hydrogenated (yellow) soluble forms of myoglobin.

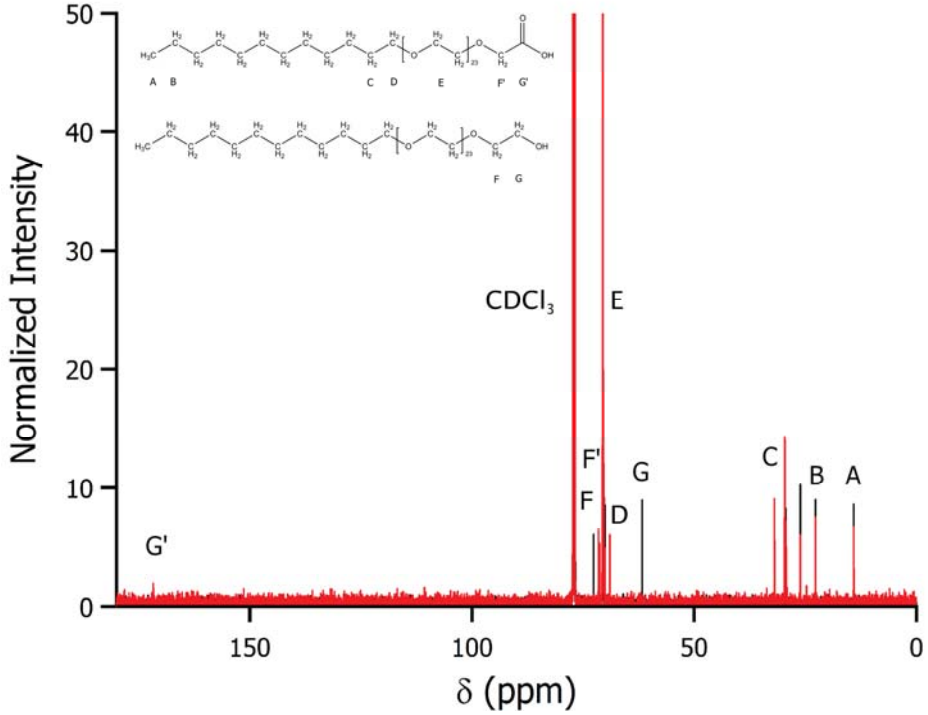

Figure SI Methods 2. ^{13}C NMR spectrum of polyoxyethylene lauryl ether (black) showing a peak at 61.84 ppm from the carbon adjacent to the terminal hydroxyl group (G). The oxidation of the alcohol to yield glycolic acid ethoxylate lauryl ether (HS_5) gave a ^{13}C NMR spectrum (red) with no feature at 61.84 ppm, and a small peak at 171.85 ppm (G′) corresponding to carboxylate carbon.

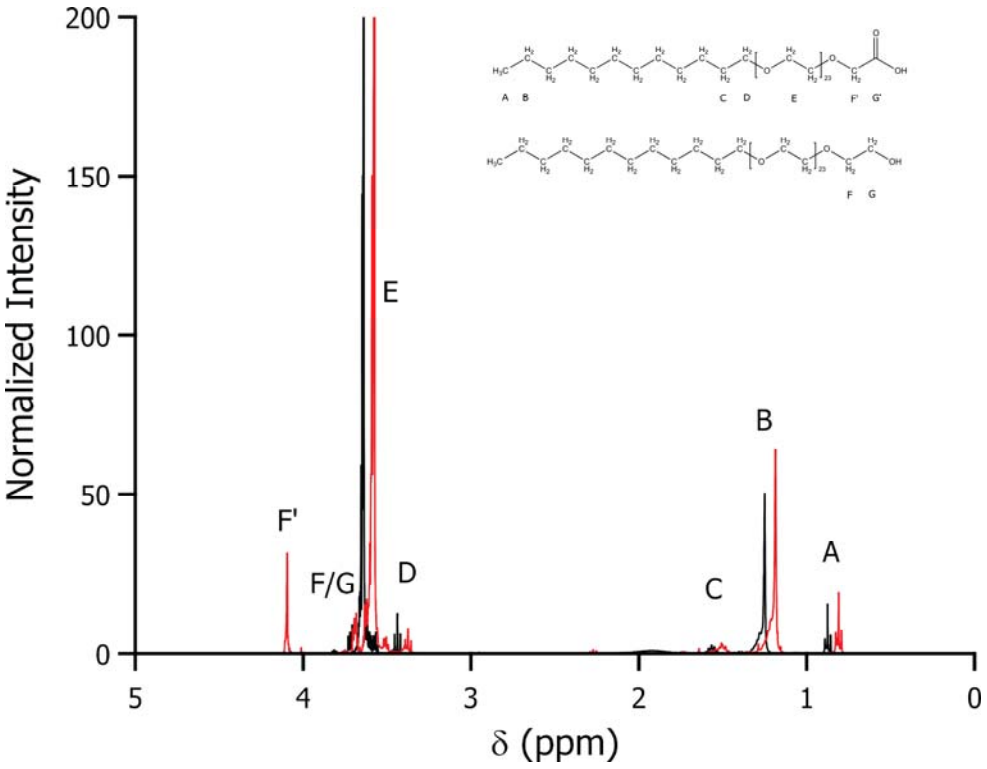

Figure SI Methods 3. ^{1}H NMR spectrum of glycolic acid ethoxylate lauryl ether (**HS_5**) (red) showing effective oxidation of polyoxyethylene lauryl ether (black) as evidenced by the formation of a peak at 4.16 ppm corresponding to the protons on the α-carbon to the carboxylate.

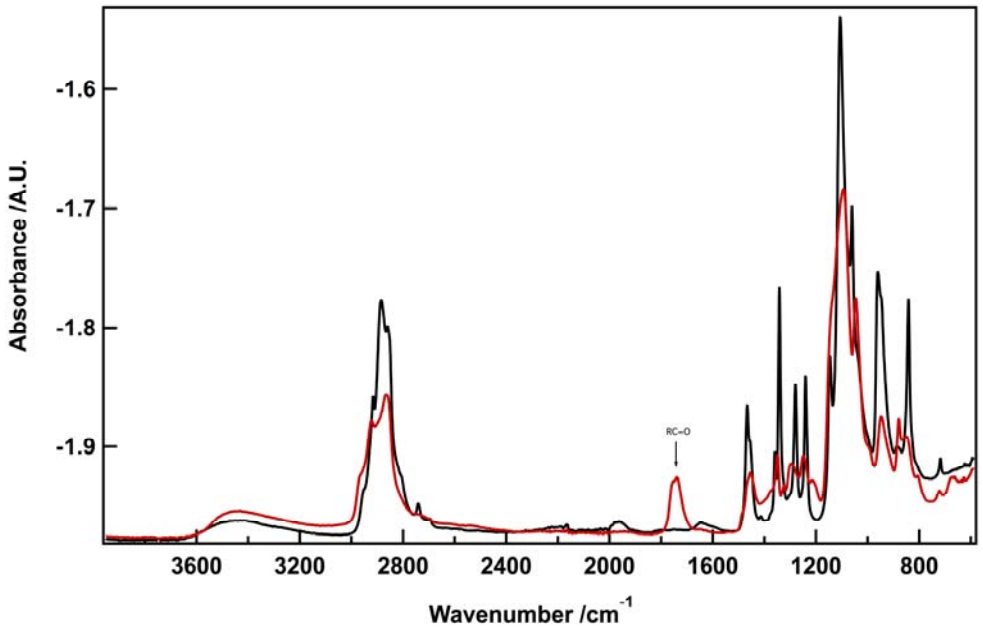

Figure SI Methods 4. FTIR spectra of polyoxyethylene lauryl ether (black) and glycolic acid ethoxylate lauryl (**HS_5**; red) showing the appearance of a strong carbonyl stretch from the carboxylic acid at 1740 cm^{-1} after oxidation.

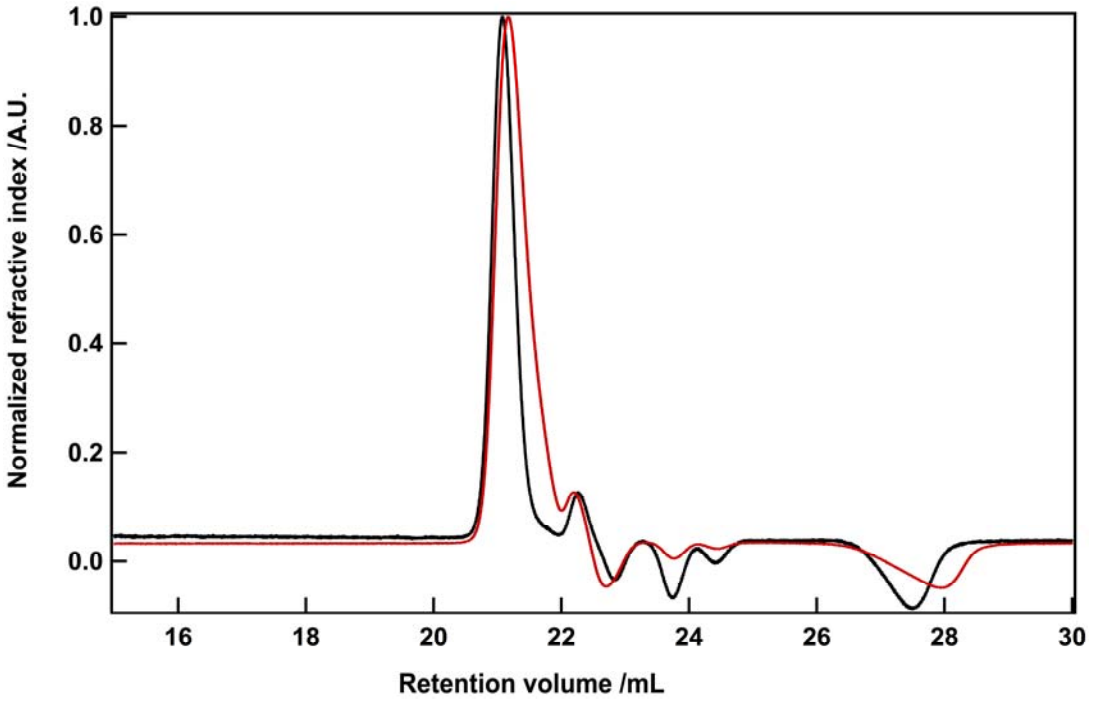

Figure SI Methods 5. Gel permeation chromatography (GPC) traces from polyoxyethylene lauryl ether (black) and glycolic acid ethoxylate lauryl **(**HS_5; red) showing almost identical retention volumes and widths, signifying no change in the polydispersity of the polymer after oxidation.

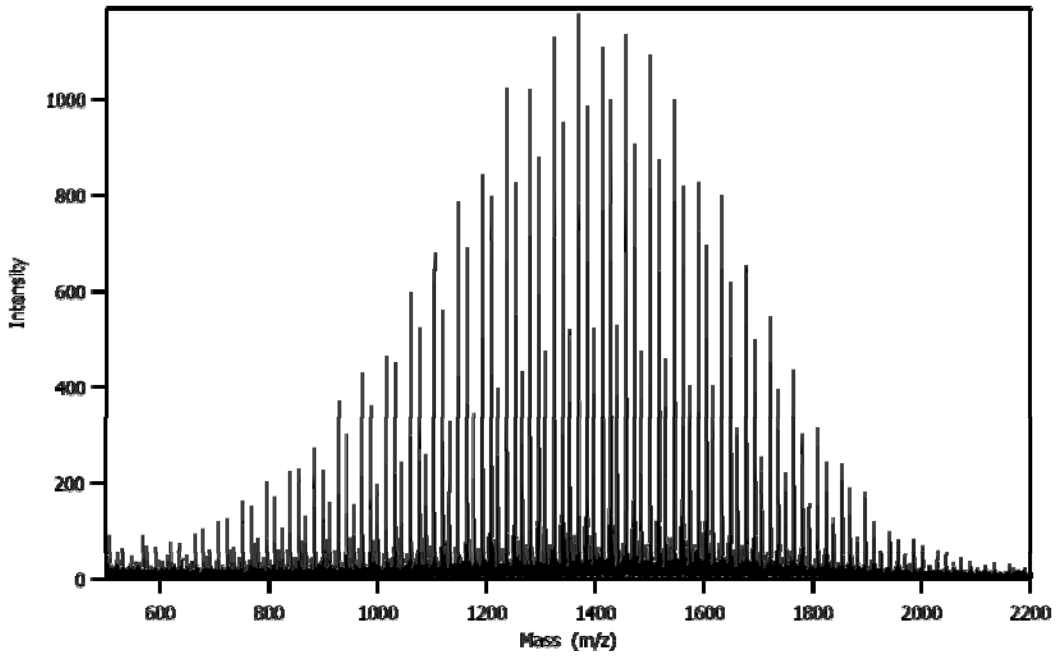

Figure SI Methods 6. MALDI mass spectrum from glycolic acid ethoxylate lauryl ether **(**HS_5**).**

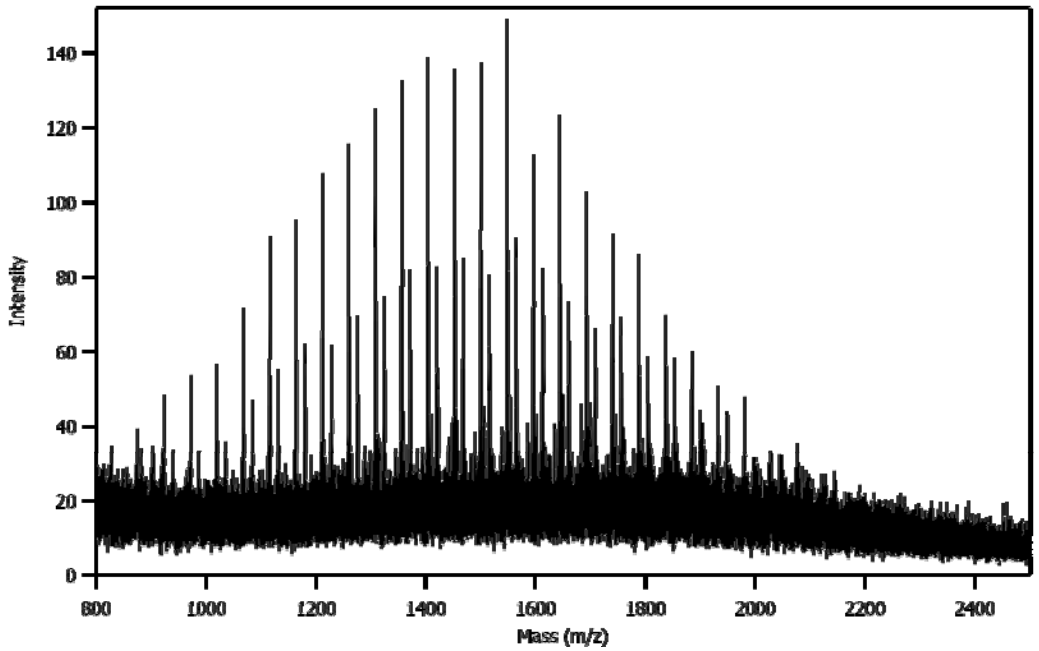

Figure SI Methods 7. MALDI mass spectrum from alpha-deuterated tridecanol propionic acid terminated deuterated poly(ethylene glycol) (DS_5).

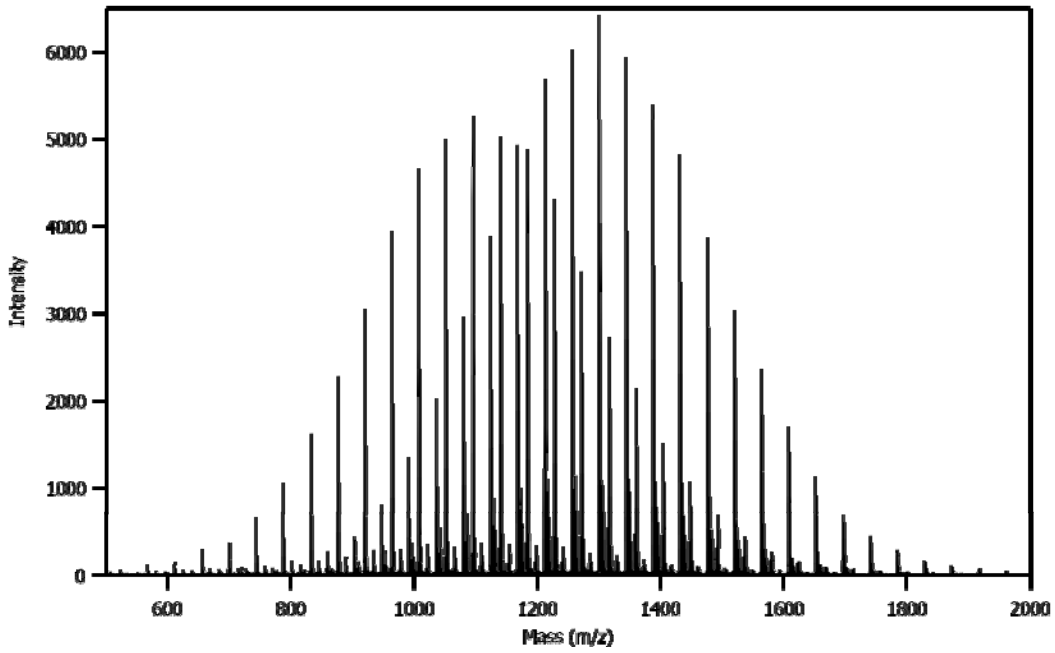

Figure SI Methods 8. MALDI mass spectrum from poly(ethylene glycol) 4-nonylphenyl 3-sulfopropyl ether (HS_1).

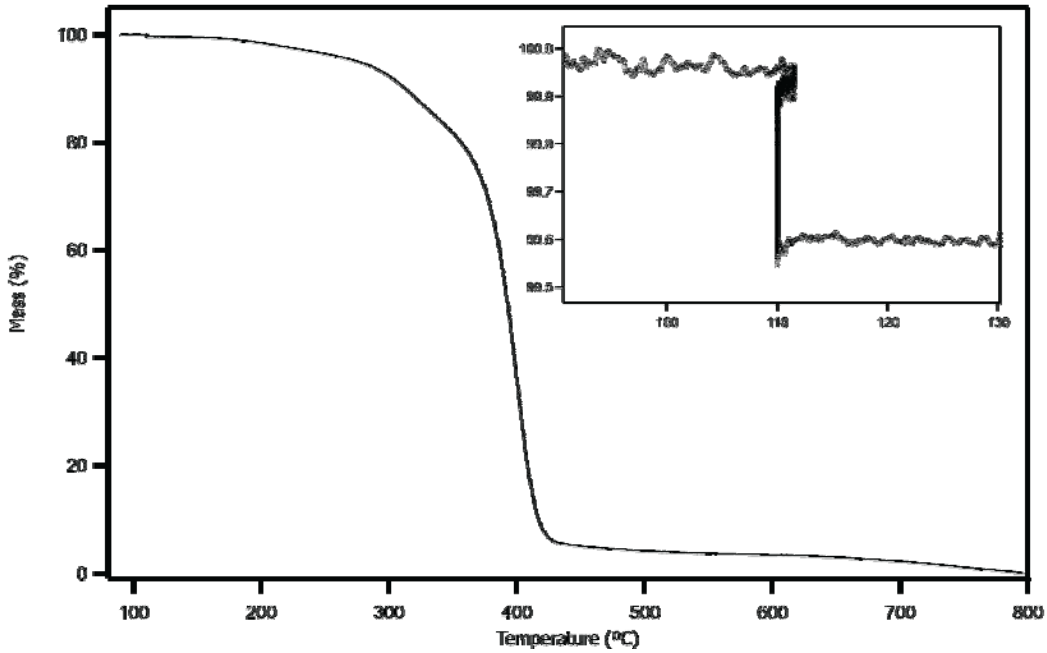

Figure SI Methods 9. Thermogravimetric analysis (TGA) of HMb/HS_5 showing a reduction in the mass as the temperature is held at 110°C for 1 hour before heating to 800°C. The insert shows the mass change due to the loss of water.

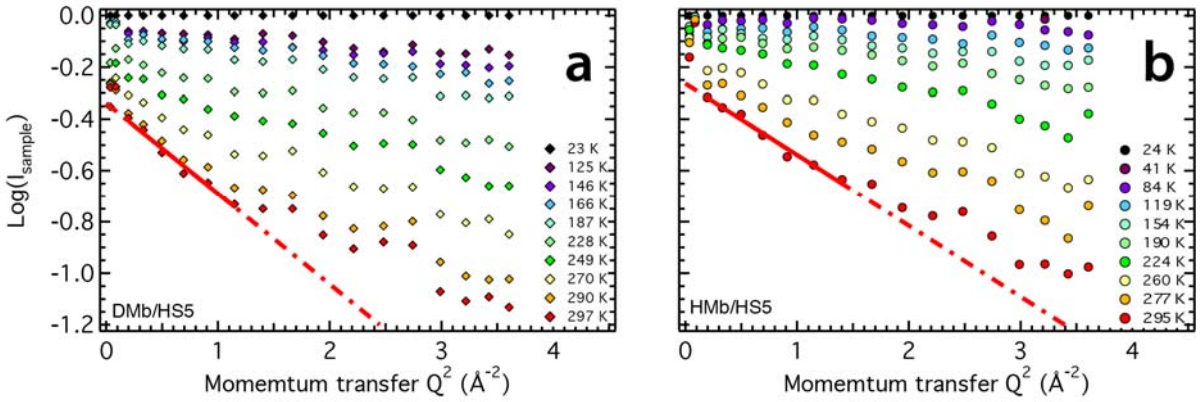

Figure SI Methods 10. Logarithms of the elastic intensities against Q^2 at selected temperatures for a) the DMb/HS_5 hybrid and b) the HMb/HS_5 hybrid. The plain red lines correspond to the linear fits used to extract the mean square displacements. The dashed red lines correspond to the extrapolation of the fits to lower and higher Q values.

2. Supporting Figures

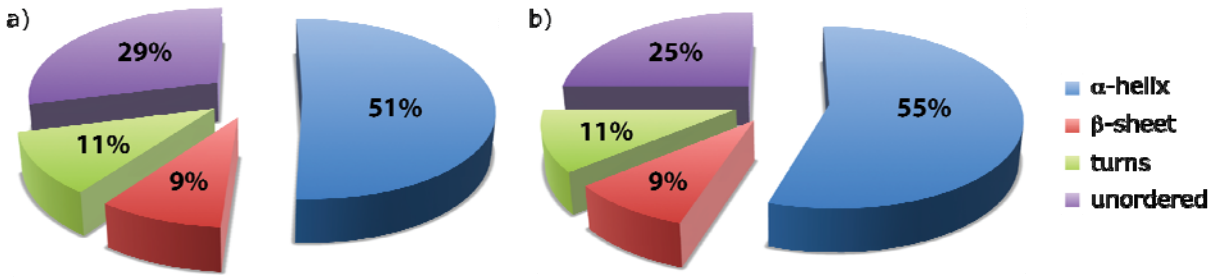

Figure S1. A comparison showing no significant variation in the SRCD-derived secondary structure contents between the hybrids a) HMb/HS_2, and b) HMb/HS_5 at 25°C.

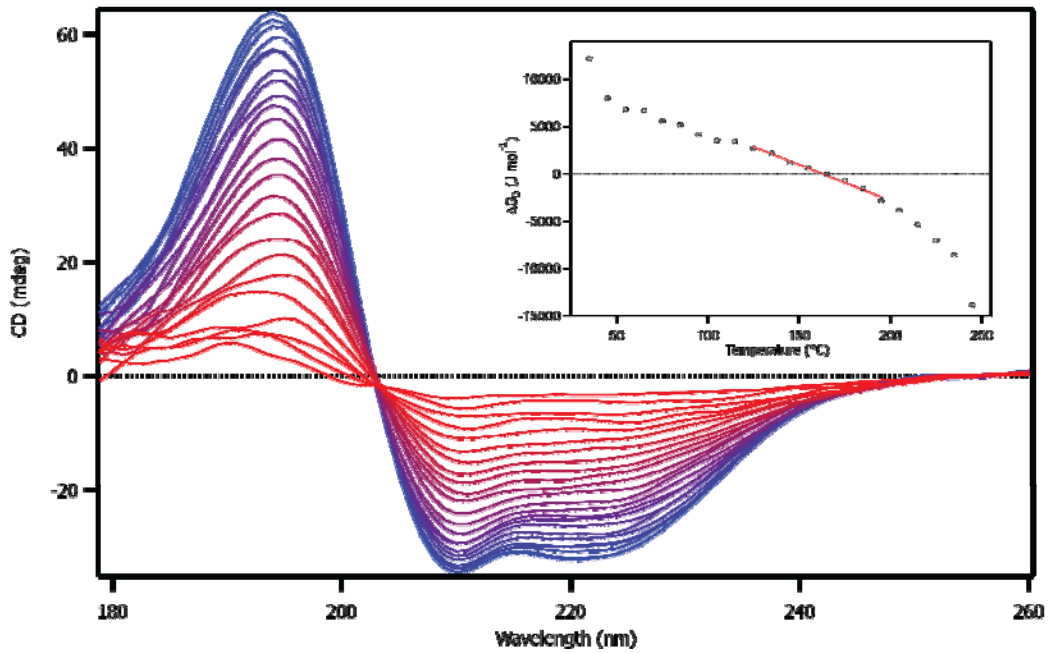

Figure S2. SRCD spectra of HMb/HS_5 in the solvent-free liquid phase showing a progressive reduction in the peak intensities at 208, 222 and 195 nm over a temperature range of 25°C (blue) to 245°C (red) at 10°C intervals. Insert shows the dependence of the free energy of denaturation (ΔG_D) on temperature.

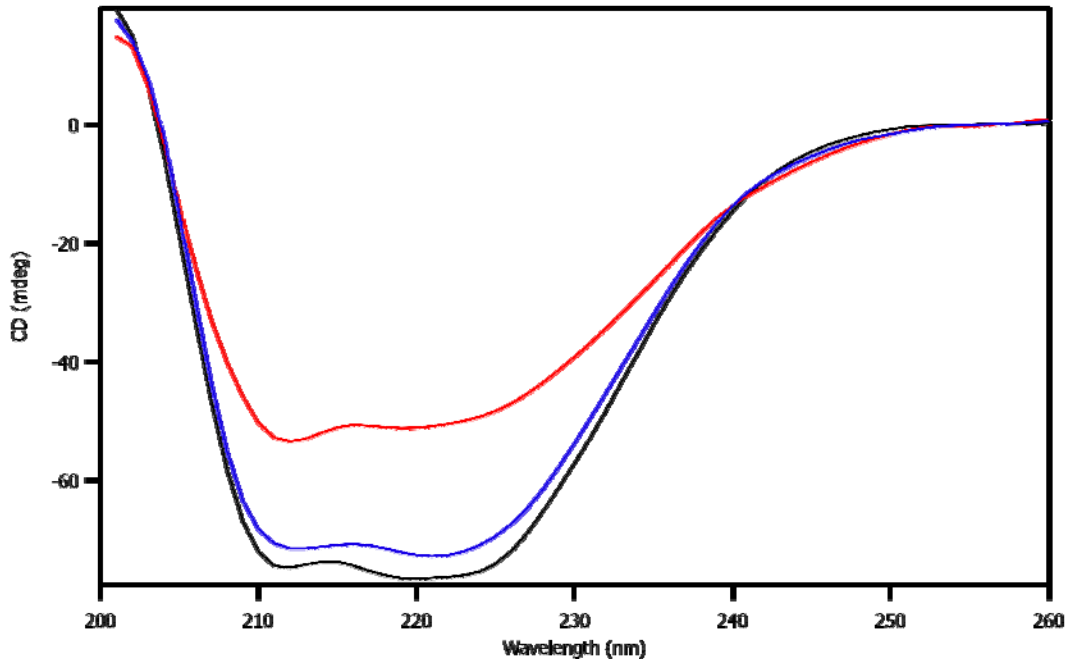

Figure S3. SRCD spectra of solvent-free liquid HMb/HS_5 at 30°C (black), after heating at 155°C (red), and after subsequent cooling at 30°C (blue). Samples were incubated for 10 minutes at each temperature.

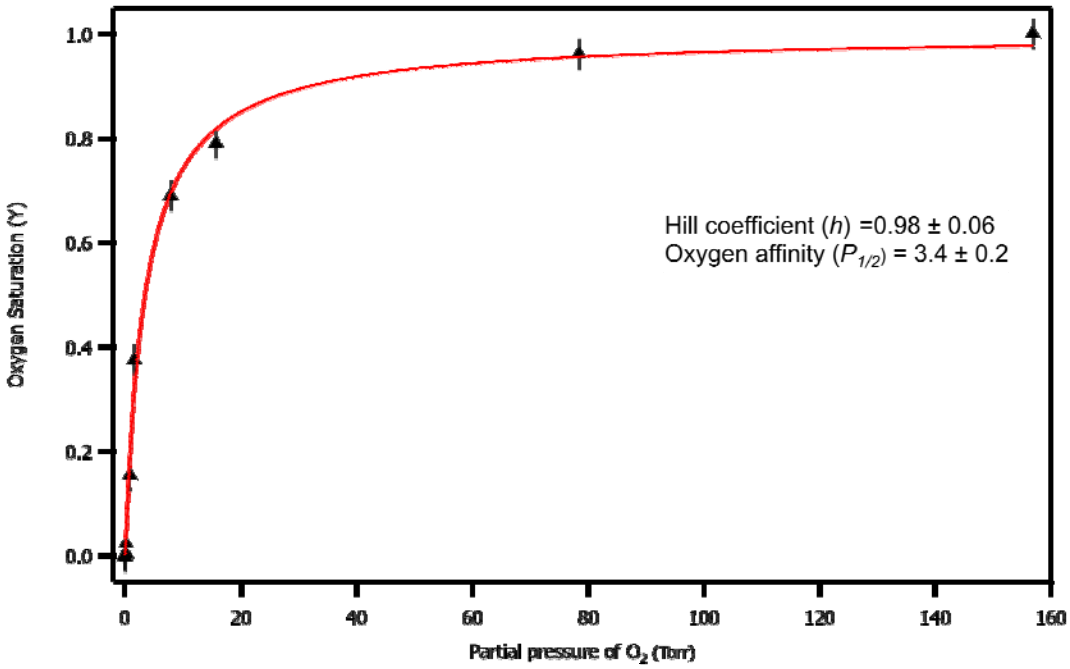

Figure S4. Equilibrium dioxygen association curve showing degree of oxygen saturation against partial pressure of dioxygen (pO_2) for HMb/HS_5 at 37°C. Data points (triangles) originated from Gaussian fits to the Soret band, and were fitted using the Hill equation (red line).

Supporting references

(1) Kataoka, M.; Nishii, I.; Fujisawa, T.; Ueki, T.; Tokunaga, F.; Goto, Y. *J Mol Biol* **1995**, *249*, 215.
(2) Stadler, A. M.; Pellegrini, E.; Johnson, M.; Fitter, J.; Zaccai, G. *Biophys J* **2012**, *102*, 351.
(3) Araki, J.; Zhao, C. M.; Kohzo, I. *Macromolecules* **2005**, *38*, 7524.
(4) Perriman, A. W.; Brogan, A. P.; Colfen, H.; Tsoureas, N.; Owen, G. R.; Mann, S. *Nat Chem* **2010**, *2*, 622.
(5) Dolman, M.; Halling, P. J.; Moore, B. D.; Waldron, S. *Biopolymers* **1997**, *41*, 313.
(6) Frick, B.; Gonzalez, M. *Physica B: Condensed Matter* **2001**, *301*, 8.
(7) Gallat, F.-X.; Laganowski, A.; Wood, K.; Gabel, F.; van Eijck, L.; Wuttke, J.; Moulin, M.; Härtlein, M.; Eisenberg, D.; Colletier, J.-P.; Zaccai, G.; Weik, M. *Biophys J* **2012**, *103*, 129.
(8) Wuttke, J.; Budwig, A.; Drochner, M.; Kämmerling, H.; Kayser, F.-J.; Kleines, H.; Ossovyi, V.; Pardo, L. C.; Prager, M.; Schneider, G. J.; Schneider, H.; Staringer, S.; Richter, D. *Rev. Sci. Instr.* **2012**, *in press*, .
(9) Whitmore, L.; Wallace, B. A. *Nucleic Acids Res.* **2004**, *32*, W668.
(10) Sreerama, N.; Woody, R. W. *Anal. Biochem.* **2000**, *287*, 252.
(11) Lees, J. G.; Miles, A. J.; Wien, F.; Wallace, B. A. *Bioinformatics* **2006**, *22*, 1955.
(12) Whitmore, L.; Wallace, B. A. *Biopolymers* **2008**, *89*, 392.
(13) Pace, C. N. *Critical Reviews in Biochemistry* **1975**, *3*, 1.
(14) Sinha, A.; Yadav, S.; Ahmad, R.; Ahmad, F. *Biochem. J.* **2000**, *345*, 711.
(15) Taneja, S.; Ahmad, F. *Biochem. J.* **1994**, *303*, 147.